journal

J. Am. Ceram. Soc., 83 [2] 436–38 (2000)

Recrystallization of Oxygen Ion Implanted $Ba_{0.7}Sr_{0.3}TiO_3$ Thin Films

R. Liedtke,† S. Hoffmann,‡ and R. Waser*,†,‡

IWE II, RWTH Aachen University of Technology, D-52056 Aachen, Germany

IFF, Forschungszentrum Jülich, D-52425 Jülich, Germany

The crystallization behavior of chemical-solution-deposited and amorphous $Ba_{0.7}Sr_{0.3}TiO_3$ (BST) thin films was analyzed with respect to the evolution of the structural and dielectric properties of the films as a function of the annealing temperature. The amorphous films were produced by oxygen ion implantation into crystalline BST thin films. In the amorphous thin films, the crystallization to the perovskite phase occurred at $T = 550$°C, whereas the as-deposited CSD films showed the first crystalline XRD-reflex only after annealing at $T = 650$°C. Here a carbon-rich intermediate phase delayed the crystallization process to higher temperatures.

I. Introduction

ELECTROCERAMIC thin films exhibit an increasing interest due to their possible integration into the silicon circuit technology. Nonferroelectric, high-permittivity ceramic thin films of $Ba_{0.7}Sr_{0.3}TiO_3$ (BST) find potential use in integrated capacitors and dynamic random access memories (DRAMs).[1] The thin films can be deposited at temperatures compatible to the silicon technology by a variety of methods, e.g., physical vapor deposition techniques,[2] chemical vapor deposition (MOCVD),[3] or chemical solution deposition (CSD).[4,5,6,7] CSD is widely used as a relative easy and flexible technique for the thin film preparation. While the CSD technique most probably is not suitable for submicrometer size ultra-large-scale integration (ULSI) as required for future DRAM generations, integration of decoupling and filter capacitors remains an attractive issue.[8]

During several back end process steps like reactive ion etching (RIE) or the deposition of the metal top electrodes by sputtering, crystal defects are generated within the ceramic film. The removal of such defects is very important to enhance the electrical properties of the fully processed device. Therefore, the elimination of crystal defects during the recryallization of BST thin films has been considered in this project.

In the present paper a detailed comparative study of the evolution of the structural and dielectric properties of (1) CSD-derived and (2) amorphous BST thin films during crystallization will be reported.

II. Experimental Procedure

The CSD route applied for this study was the propionate route because of its flexibility with respect to the choice of the elements.[4] The starting materials were barium propionate $[Ba(CH_3CH_2COO)_2]$, strontium propionate $[Sr(CH_3CH_2COO)_2]$, and titanium tetra-*n*-butoxide (TBT) $[Ti(C_4H_9O)_4]$. Propionic acid $[CH_3CH_2COOH]$ and 1-butanol $[CH_3(CH_2)_3OH]$ were used as solvents. Additionally the TBT was stabilized against hydrolysis with acetylacetone (Hacac) in molar ratio of 1:2. The resulting solution was diluted to achieve a concentration of 1.0*M*. Hoffman *et al.*[5] have shown that a diluted precursor favors a dense, columnar structured growth of the BST thin films. The filtered BST solutions were deposited on platinized Si wafters ($Pt/TiO_x/SiO_2/Si$) by spin-coating at 4000 rpm for 30 s. The wet coatings were pyrolyzed on a hot plate at 200°C in air and were subsequently annealed in a Rapid Thermal Anneal System (RTA) for 3 min in a 1 bar oxygen atmosphere. The RTA temperature was varied from $T = 430$°C to 800°C. The spin-coating and heating procedure was repeated for 16 times to achieve BST films with a thickness of 130 nm after crystallization.

A set of crystalline BST thin films was prepared at $T = 750$°C as described above, and was subsequently amorphized by adequate oxygen ion implantation. A total dose of $N(O^+) = 2 \times 10^{16}$ cm^{-2} and various energies ranging from $E = 50$ keV up to 200 keV were chosen. During the implantation the samples were held at room temperature. These samples were annealed in the RTA at temperatures ranging from $T = 500$°C up to 800°C for 3 min. After the first characterization the films were postannealed at the corresponding temperatures in a furnace for 2 h. The structure of the films was investigated using X-ray diffraction analysis (XRD) in grazing incidence, and the morphology was studied by scanning electron microscopy (SEM). Platinum top electrodes with an area of 1 mm^2 were deposited by dc magnetron sputtering through a shadow mask. The capacitance was measured at a frequency of 10 kHz using a HP 4284A impedance analyzer with a signal of $V_{RMS} = 30$ mV.

III. Results and Discussion

(1) Structural Characterization

The crystalline nature of the films was identified by XRD. Figure 1(a) shows the XRD pattern of the CSD-derived films for different annealing temperatures ranging from $T = 430$°C to 700°C. At $T = 430$°C no peaks of the crystalline $Ba_{0.7}Sr_{0.3}TiO_3$ phase can be detected; only the wafer peaks are present. The broad peak at about $2\theta = 27°$ stems from an intermediate phase. Up to temperatures of about $T = 650$°C peaks of the intermediate, nonperovskite phase at 2θ values of 27.2° and 35.0° sharpen and completely disappear at $T = 700$°C. This intermediate phase, which is indicated by C in Fig. 1(a), can be identified as the alkaline-earth oxocarbonate phase detected for the first time by Gopalakrishnamurthy *et al.*[9] Hennings *et al.*[10] attributed the stoichiometry $Ba_2Ti_2O_5CO_3$ to this phase. The present studies show that this intermediate phase is stable up to $T = 600$°–650°C in the thin films. For the CSD-prepared BST films the single crystalline perovskite phase is first observed at $T = 650$°–700°C depending on the annealing time.

H.U. Anderson—contributing editor

Manuscript No. 189236. Received August 24, 1999; approved October 28, 1999

*Member, American Ceramic Society.
†RWTH Aachen University of Technology.
‡Forschungszentrum Jülich.

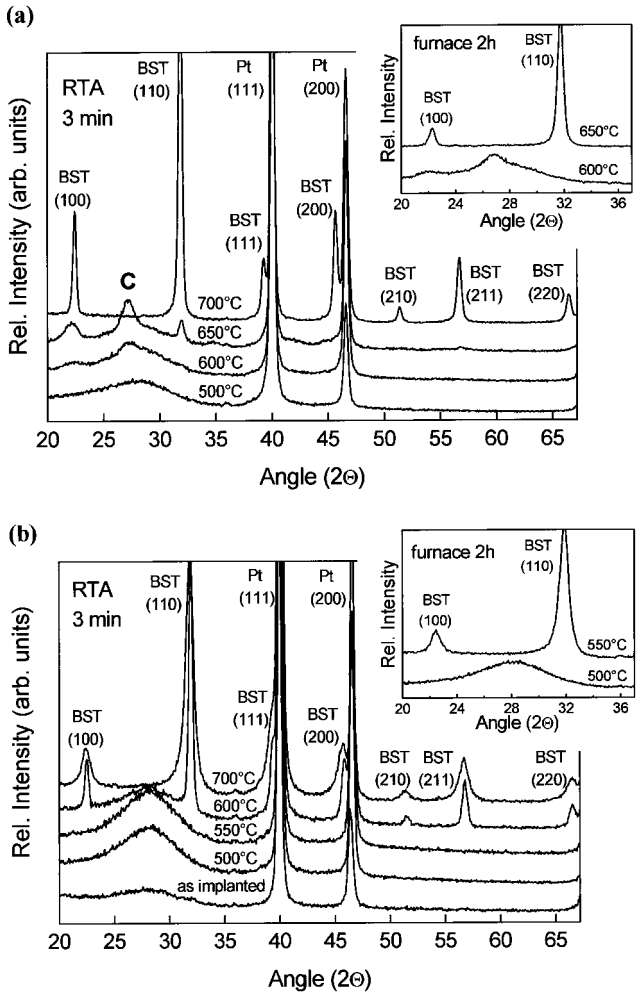

Fig. 1. XRD pattern of BST thin films prepared at different temperatures: (a) CSD-derived and (b) recrystallized BST thin films. The insets show the XRD diagrams of the postannealed samples.

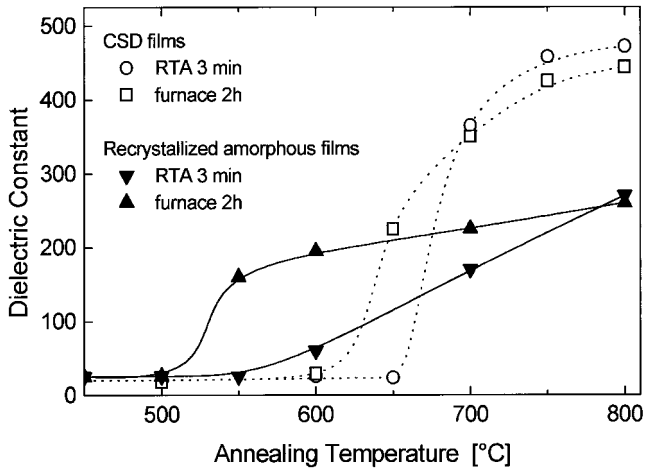

Fig. 2. Permittivity of BST thin films as a function of the annealing temperature. The experimental data show that the recrystallized samples never reach the dielectric constant of the CSD-derived thin films. The lines are guides for the eye.

In order to study the crystallization behavior of carbon-free amorphous BST thin films, crystalline BST films which had been annealed at 750°C were completely amorphized by oxygen ion implantation. The impact of the implanted oxygen ions causes a destruction of the crystal structure, which is indicated by the absence of the perovskite reflexes in the XRD diagram shown in Fig. 1(b). Because of the very high ionicity (>80%) of the BST thin films, it is supposed that such material does not form a network and the amorphous structure is a dense random packaging of hard spheres (DRPHS model).[11] The XRD patterns of the differently annealed samples are shown in Fig. 1(b). For temperatures below $T = 600$°C a broad peak at about $2\theta = 27°$ develops, which reaches an intensity maximum at $T = 550$°C. At $T = 600$°C this peak decreases, whereas at the same time clear diffraction patterns of the perovskite structure appear. By postannealing for 2 h the perovskite crystallization temperature can be reduced to $T = 550$°C (inset of Fig. 1(b)).

(2) Dielectric Properties

The permittivity of BST thin films depends strongly on the film density, the thickness,[12] and the grain size.[13] As the columnar microstructure is characterized by grains proceeding through the whole film thickness it typically results in higher values of the permittivity than a small grain morphology.[5]

The aim of the electrical characterization is to relate the dielectric permittivity to the structural properties of the BST thin films. Figure 2 shows the permittivity as a function of the annealing temperature and time of the CSD-derived and recrystallized BST thin films. Samples annealed at a temperature of up to $T = 650$°C show a small permittivity of $\varepsilon_r \approx 25$, which indicates the low permittivity of the intermediate phase or the one of the carbon-rich films, respectively. About $T = 700$°C, where the perovskite phase develops, the permittivity increases rapidly. The dependence of the permittivity values on the annealing temperature and time follows exactly the crystallization of the perovskite phase as observed by XRD. This underlines that an annealing temperature of at least $T = 650$°C is necessary to form the perovskite structure in the CSD-derived BST thin films within reasonable times.

Additionally Fig. 2 shows the corresponding permittivities of the amorphized BST samples annealed for 3 min and 2 h, respectively. Up to an annealing temperature of $T \leq 500$°C the permittivity is low ($\varepsilon_r \approx 25$). In the case of the samples annealed for 3 min a nearly linear increase of the permittivity is observed with increasing annealing temperature. The 2 h postannealed samples show a clear step in the permittivity as a function of the annealing temperature. If the temperature is raised above $T = 550$°C, the permittivity increases rapidly from $\varepsilon_r = 25$ to $\varepsilon_r = 175$. Further increase of the annealing temperature leads to a small increase in the permittivity, which is attributed to a slight grain growth in the BST thin films. At a temperature of $T = 800$°C the curves of the short-time-annealed and postannealed samples are nearly identical, which indicates that a complete recrystallization has occurred at $T = 800$°C within 3 min.

In order to confirm the correlation between the observed crystallization behavior and the dielectric properties found in the prepared BST thin films, the microstructures of the ceramic thin films were studied by means of scanning electron microscopy (SEM). The SEM micrographs of the CSD-derived films, which were annealed at $T \geq 700$°C, reveal a columnar microstructure (Fig. 3(a)). Figure 3(b) shows that the oxygen ion implantation completely amorphized the film. In Fig. 3(c) the microstructure of a recrystallized film is shown which consists of very fine grains. The columnar microstructure is no longer present, which indicates a completely new formation of the microstructure after recrystallization at $T = 700$°C.

IV. Conclusions

The crystallization behaviors of CSD-derived and amorphous BST films have been found to differ significantly. For the CSD thin films a metastable, carbon-rich intermediate phase delays the crystallization point to higher temperatures. If the annealing temperature is raised above $T = 700$°C, the remaining carbonate is

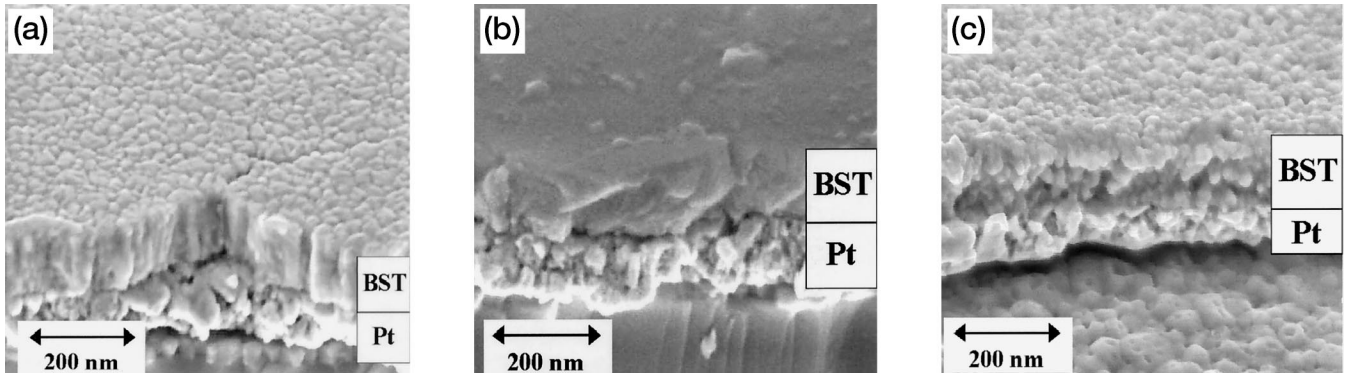

Fig. 3. SEM micrographs of BST thin films: (a) BST thin film prepared by CSD at $T = 700°C$, (b) amorphized BST thin film by oxygen ion implantation, (c) recrystallized thin film from the amorphous phase at $T = 750°C$.

eliminated and a columnar microstructure of the films develops due to layer-by-layer epitaxy. In contrast the BST thin films recrystallized from an amorphous phase exhibit a very small-grained microstructure, which probably develops because of homogeneous nucleation of small nanocrystals in the amorphous thin film. Because of the low recrystallization temperature of about $T = 550°C$, which is in the range of only one third of the melting temperature of BST, long-range mass transport during annealing is strongly inhibited[14] and therefore no significant grain growth can occur. The crystallization temperature of the BST thin films found in our investigations is in good agreement with those found by Noh *et al.*[15] for sputtered BST films on MgO substrates. The metastable pyrochlore phase identified by Noh is not observed in our films. The differences in the average grain size of the CSD-derived and recrystallized thin films are most probably responsible for the lower permittivity of the recrystallized films in comparison to CSD-derived ones.

The recrystallization temperature of BST thin films is important for further process development concerning the integration of BST thin films into the silicon technology. During several process steps defects are generated in the BST films due to the impact of high-energy ions. The amorphized films used in this study may represent the worst case of a damaged crystal structure that can occur during the device processing mentioned above. An annealing step with a recrystallization temperature of $T = 550°–600°C$ can be used mainly to eliminate the produced crystal defects. Unfortunately, the recrystallized BST thin films in our study revealed inferior electrical properties than the as-deposited films, which is attributed to the fine-grained microstructure. Therefore, process steps following BST thin film deposition have to be applied carefully with respect to the induced crystal damage.

Acknowledgment

We are grateful to W. Michelsen (Institut for Thin Film and Ion Technology, Research Center Jülich) for performing the ion implantation.

References

[1]P.-Y. Lesaicherre, H. Yamaguchi, Y. Miyasaka, H. Watanabe, H. Ono, and M. Yoshida, "$SrTiO_3$ Thin Films by MOCVD for 1 Gbit DRAM Application," *Integr. Ferroelectr.*, **8**, 201–25 (1995).

[2]B. Panda, A. Dhar, G. D. Nigam, D. Bhattacharya, and S. K. Ray, "Relationship between Plasma Parameters and Film Microstructure in Radio Frequency Magnetron Sputter Deposition of Barium Strontium Titanate," *J. Appl. Phys.*, **83** [2] 1114–19 (1998).

[3]G. W. Dietz, M. Schumacher, R. Waser, S. K. Streiffer, C. Basceri, and A. I. Kingon, "Leakage Currents in $Ba_{0.7}Sr_{0.3}TiO_3$ Thin Films for Ultrahigh-Density Dynamic Random Access Memories," *J. Appl. Phys.*, **82** [5], 2359–64 (1997).

[4]U. Hasenkox, S. Hoffman, and R. Waser, "Influence of Precursor Chemistry on the Formation of $MTiO_3$ (M = Ba, Sr) Ceramic Thin Films," *J. Sol–Gel Sci. Technol.*, **12**, 67–79 (1998).

[5]S. Hoffman, U. Hasenkox, R. Waser, C. L. Jia, and K. Urban, "Chemical Solution Deposited $BaTiO_3$ and $SrTiO_3$ Thin Films with Columnar Microstructure," *Mater. Res. Soc. Symp. Proc.*, **474**, 9–14 (1997).

[6]B. A. Baumert, L.-H. Chang, A. T. Matsuda, C. J. Tracy, N. G. Cave, R. B. Gregory, and P. L. Fejes, "A Study of Barium Strontium Titanate Thin Films for Use in Bypass Capacitors," *J. Mater. Res.*, **13**, 197–204 (1998).

[7]A. S. Shaikh and G. M. Vest, "Kinetics of $BaTiO_3$ and $PbTiO_3$ Formation from Metallo-organic Precursors," *J. Am. Ceram. Soc.*, **69** [9] 682–88 (1986).

[8]K. Arita, E. Fujii, Y. Shimada, Y. Uemoto, T. Nasu, A. Inoue, A. Matsuda, T. Otsuki, and N. Suzuoka, "Si LSI Process Technology for Integrating Ferroelectric Capacitors," *Jpn. J. Appl. Phys.*, **33**, 5397–99 (1994).

[9]H. S. Gopalakrishnamurthy, M. Subba Rao, and T. R. Narayana Kutty, "Thermal Decomposition of Titanyl Oxalates—I. Barium Titanyl Oxalate; II. Kinetics of Decomposition of Barium Titanyl Oxalate," *J. Inorg. Nucl. Chem.*, **37**, 891–98 (1975).

[10]D. Hennings, G. Rosenstein, and S. Schreinemacher, "Hydrothermal Preparation of Barium Titanate from Barium-Titanium Acetate Gel Precursor," *J. Eur. Ceram. Soc.*, **8**, 107–15 (1991).

[11]A. Onton and V. Marelle, "Structure and Excitation of Amorphous Solids," *AIP Conf. Proc.*, **31**, 320–23 (1976).

[12]M. H. Frey, Z. Xu, P. Han, and D. A. Payne, "The Role of Interfaces on an Apparent Grain Size Effect on the Dielectric Properties of Ferroelectric Barium Titanate Ceramics," *Ferroelectrics*, **206–207**, 337–53 (1989).

[13]G. Arlt, D. Hennings, and G. de With, "Dielectric Properties of Fine-Grained Barium Titanate Ceramics," *J. Appl. Phys.*, **58**, 1619–25 (1985).

[14]P. A. Langjahr, T. Wagner, M. Rühle, and F. F. Lange, "Epitaxial Growth and Structure of Cubic and Pseudocubic Perovskite Films on Perovskite Substrates," *Mater. Res. Soc. Symp. Proc.*, **401**, 109–14 (1996).

[15]D. Y. Noh, H. H. Lee, J. H. Je, and H. K. Kim, "Crystallization of Amorphous (Ba,Sr)TiO_3/MgO(001) Thin Films," *Appl. Phys. Lett.*, **72** [22], 2823–25 (1998). □